Iran. J. Radiat. Res., 2010; 7 (4): 201-206

Individual virtual phantom reconstruction for organ dosimetry based on standard available phantoms

F. Babapour Mofrad[1*], R. Aghaeizadeh Zoroofi[2], A. Abbaspour Tehrani Fard[1,3], Sh. Akhlaghpoor[4], Y.W. Chen[5], Y. Sato[6]

[1]Faculty of Engineering, Science and Research Branch, Islamic Azad University, Tehran, Iran
[2]Control and Intelligent Processing Center of Excellence, School of Electrical and Computer Engineering, College of Engineering, University of Tehran, Tehran, Iran
[3]Electrical and Electronic Engineering School, Sharif University of Technology, Tehran, Iran
[4]Department of Interventional Radiology, Sina Hospital, Tehran University of Medical Sciences, Tehran, Iran
[5]College of Information and Science, Ristumeikan University, Shiga, Japan
[6]Division of Image Analysis, Graduate School of Medicine, Osaka University, Osaka, Japan

Background: In nuclear medicine application often it is required to use computational methods for evaluation of organ absorbed dose. Monte Carlo simulation and phantoms have been used in many works before. The shape, size and volume in organs are varied, and this variation will produce error in dose calculation if no correction is applied. ***Materials and Methods:*** A computational framework for constructing individual phantom for dosimetry was performed on five liver CT scan data sets of Japanese normal individuals. The Zubal phantom was used as an original phantom to be adjusted by each individual data set. This registration was done by Spherical Harmonics (SH) and Thin-Plate Spline methods. Hausdorff distance was calculated for each case. ***Results:*** Result of Hausdorff distance for five individual phantoms showed that before registration ranged from 140.9 to 192.1, and after registration it changed to 52.5 to 76.7. This was caused by index similarity ranged from %56.4 to %70.3. ***Conclusion:*** A new and automatic three-dimensional (3D) phantom construction approach was suggested for individual internal dosimetry simulation via Spherical Harmonics (SH) and Thin-Plate Spline methods. The results showed that the individual comparable phantom can be calculated with acceptable accuracy using geometric registration. This method could be used for race-specific statistical phantom modeling with major application in nuclear medicine for absorbed dose calculation. **Iran. J. Radiat. Res., 2010; 7 (4): 201-206**

Keywords: *Dosimetry, individual phantom, thin-plate spline, Monte Carlo simulation, spherical harmonics.*

INTRODUCTION

Monte Carlo (MC) is powerful and well-known numerical technique for solving statistical problems in nuclear medicine. The mathematical human phantoms are used for sampling of radionuclide distribution in two different principles (analytical description of a source, and second pixel-based image) [1-3]. Nuclear medicine phantoms have been widely used for quality control, estimation of organ dose and other dosimetric purposes [4].

To reach the more realistic human anatomy, the tomographic phantoms from segmented computed tomography (CT) or magnetic resonance images (MRI) were developed [2] such as Zubal phantoms [3]. Recently new racial phantoms have been developed [2, 4].

The best approach for precise organ dose calculation will be achievable by individual organ reconstruction. However adopting simulation computational models in radiation dosimetry such as Mont Carlo codes is also necessary. In this study, it has been tried to modify a standard phantom according to individual organ data derived from CT images, in order to simplify application of the standard phantom.

Many robust methods for shape modeling and 3-D processing are used: Spherical Harmonics shape description (SPHARM) [5] was used for surface modeling and a

Corresponding author:
Farshid Babapour Mofrad,
Faculty of Engineering, Science and Research Branch,
Islamic Azad University, Tehran, Iran.
Fax: *+98 21 44869656*
E-mail: *farshid.mofrad@yahoo.com*

non-rigid point matching for landmark tagging and the least square method and Thin-Plate Spline (TPS) [6] for registration. The two major advantages of this method are to create different comparable phantoms (necessary to enhance the total evaluation based on statistical validation) and to increase the accuracy in case study simulation.

MATERIALS AND METHODS

The data sets were acquired by a GE multi detector CT scanner at Osaka University Medical School from normal cases between 50-75 years. The imaging system parameters were as follows: in-plane resolution: 1.25 × 1.25 mm^2; inter-slice resolution: 2.5 mm; image-dimension: 512 × 512 pixels. We randomly selected five datasets for analysis. The ranges of the liver slices for data sets were between 119 to 149 slices. There was no previous assumption on the shape, size, location, and intensity range of livers.

It is necessary to have a brief introduction about Zubal phantom which is used as a template in this study. Then, we explain a novel automatic alignment method for constructing the individual comparable phantom based on coherent point drift (CPD) [7, 8] and spherical harmonics shape descriptors [5] which is a mathematical powerful tool for analyzing and synthesizing the closed surfaces and human object shapes.

Preprocessing on Zubal Phantom and data sets

Zubal phantom have been widely used for dose estimation and other nuclear medicine application. In this study we have used a Zubal phantom in dimensions 128×128×243 and one byte array. The segmented liver was selected in the phantom and then further processing was necessary for extracted binary images to remove holes and obtain a smooth and standard mesh (figure 1).

In CT scan images, the boundaries of the segmented livers were employed for liver surface approximation. In each slice, the liver boundary was manually determined by the expert. The sample boundary points for each case were determined by considering all boundary points of all slices. Further processing [12] including smoothing, dilation and erosion, filling was essential, in most cases after extracting liver.

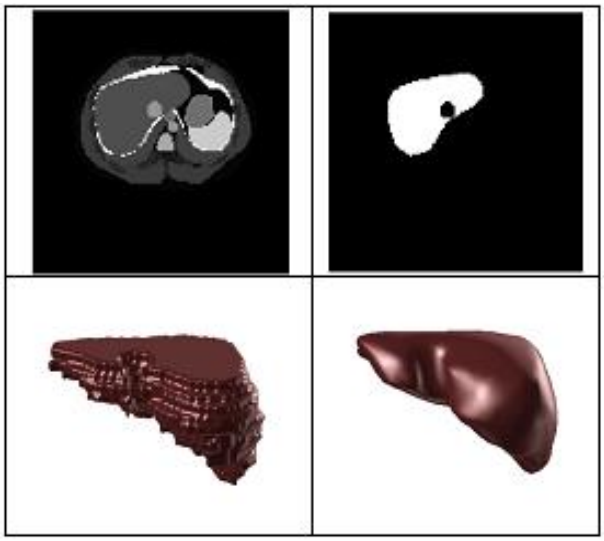

Figure 1. One slice of zubal phantom and liver segmented in binary image (top), and liver surface from zubal phantom without and with necessary processing (bottom).

The proposed algorithm for the construction individual phantoms was as follow:

- Automatic Space Registration
  - Object to phantom is registered in space domain
- Surface Parameterization
  - Surface was converted to uniform sphere
- Surface Expansion by Spherical Harmonics
  - S.H parameters were calculated
- Parameter Space Registration
  - Object to phantom was registered in parameter domain
- Selecting the Landmark in Phantom and Object
  - Landmark automatic was selected
- Applying Thin-Plate Spline
  - Individual phantom was prepared

Automatic object space registration

We used the coherent point drift point set registration [7, 8] based on maximum likelihood (ML) estimation problem with motion coherence constraint where one point set moves coherently to align with the second set. The method can find both the non-rigid transformation, and correspondence between two point set without any prior knowledge of transformation.

The registration aim was to bring the livers as close as possible into template with aligning the rotation and position in shape space. To find the rotation R and translation T, first, we selected template liver. Then, six landmarks were found with following comments (which is need for least-square error minimization equation 1) [9]. The number of slices with maximum area in sagittal view, axial view, coronal view and their correspondant contours were obtained in template. After combining the contours, we got six landmarks in template. Finding the exact location of these points is not so critical, since in minimization step of the algorithm other objects would aligne to template.

After applying point matching method to each liver into template, we found correspondence points into each liver before and after applying point matching. These corresponding landmarks were obtained before and after applying point matching in R^3, then, we employed a quaternion-based algorithm to find the rotation and translation [9].

$$f(R,T) = \frac{1}{n}\sum_{i=1}^{n} \left\| q_i - Rp_i - T \right\|^2 \qquad (1)$$

Where $P = \{\vec{p}_1, \vec{p}_2, .., \vec{p}_n\}$ and $Q = \{\vec{q}_1, \vec{q}_2, .., \vec{q}_n\}$ denotes landmarks matching, before and after applying point respectively. After this step all shapes were as close as possible to the template shape in space domain.

Spherical harmonics

This section discuss about the mathematical property of the Spherical Harmonics basis functions, Spherical Harmonics shape descriptors using parameterization of surface presented by Brechbuhler's *et al.* [10].

Surface parameterization is a step in the shape description which continues and uniforms mapping of the surface points to parameter space of a sphere. It means each point of the surface should map exactly to one point on the unit sphere [5, 10].

$$S(\theta, \phi) = \begin{pmatrix} x(\theta, \phi) \\ y(\theta, \phi) \\ z(\theta, \phi) \end{pmatrix} \qquad (2)$$

When the free variables polar angle $\theta \in [0, \pi]$, and azimuthal angle $\phi \in [0, 2\pi)$ run over the whole sphere, S (θ, ϕ) runs over the whole surface. Figure 2 shows the parameterization result.

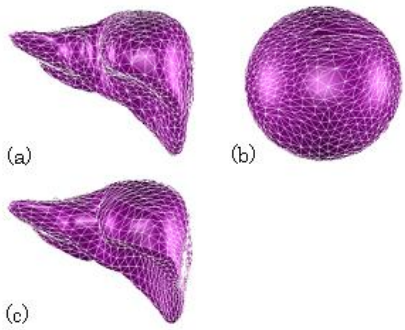

Figure 2. (a) One example of liver model with triangulated mesh. (b) Parameterization result of the object surface. (c) Reconstructed the surface of liver with Spherical Harmonics with nearly uniform sampling.

Spherical Harmonics basis functions $Y_l^m, -l \le m \le l$ of degree l and order m which are defined by the following formula:

$$Y_l^m(\theta,\phi) = \sqrt{\frac{2l+1}{4\pi}\cdot\frac{(l-m)!}{(l+m)!}} P_l^m(\cos\theta).e^{im\phi} \qquad (3)$$

$$Y_l^{-m}(\theta,\phi) = (-1)^m Y_l^{m*}(\theta,\phi) \qquad (4)$$

Where Y_l^{m*} denotes the complex conjugate o f Y_l^m and the term P_l^m is an associated Legendre polynomials function. θ is regarded as the polar (co-latitudinal) coordinate with $\theta \in [0,\pi]$, and ϕ as the azimuthal (longitudinal) coordinate with $\phi \in [0,2\pi)$.

$$P_l^m(\omega) = \frac{(-1)^m}{2^l l!}(1-\omega^2)^{\frac{m}{2}} \frac{d^{m+l}}{d\omega^{m+l}}(\omega^2-1)^l \qquad (5)$$

To represent a surface by the SPHARM, we determined the coordinate's values of the surface, i.e.,

$$S(\theta,\phi) = (x(\theta,\phi), y(\theta,\phi), z(\theta,\phi))^T$$

as follows:

$$S(\theta,\phi) = \sum_{l=0}^{\infty} \sum_{m=-l}^{l} c_l^m Y_l^m(\theta,\phi) \qquad (6)$$

The coefficients $c_l^m = (c_{xl}^m, c_{yl}^m, c_{zl}^m)^T$ are usually complex numbers, and they can be estimated by solving one set of linear equation in a least square. Each object surface can be represented by these coefficients. The approximated surface will be reconstructed with each degree of L_{max} in the following formula:

$$\hat{S}(\theta,\phi) = \sum_{l=0}^{L_{max}} \sum_{m=-l}^{l} c_l^m Y_l^m(\theta,\phi) \qquad (7)$$

The larger L_{max} (higher degree) gives more accurate and more detailed approximate surface data. Figure 3 shows an example of liver in different degree of L_{max}.

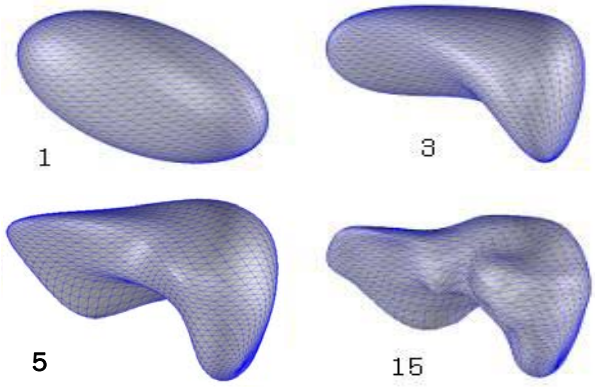

Figure 3. The Spherical Harmonics shape description of liver are shown in different degree of L_{max} (1, 3, 5 and 15).

Parameter space registration

In this Section we have explained the necessary registration steps for parameter spaces between one liver as template with others [5].

In the next step, we minimized root mean square distance $\sqrt{MSD}$ between SPHARM coefficients after rotating the parameter net on the surface in Euler angles (α, β, γ):

$$MSD = \frac{1}{4\pi} \sum_{l=0}^{L_{max}} \sum_{m=-l}^{l} \left\| c_{\mathrm{mod},l}^m - c_{tem,l}^m \right\| \qquad (8)$$

where $c_{\mathrm{mod},l}^m$, $c_{tem,l}^m$ are coefficients in each (m,l) of model and template, respectively. With following formula, having coefficients c_l^m before rotation, we can calculate the coefficients $c_l^m(\alpha,\beta,\gamma)$ after rotation with Euler angles (α, β, γ):

$$c_l^m = \sum_{n=-l}^{l} D_{mn}^l(\alpha,\beta,\gamma)\, c_l^n \qquad (9)$$

$$\begin{pmatrix} \tilde{c}_0^0 \\ \tilde{c}_1^{-1} \\ \tilde{c}_1^0 \\ \tilde{c}_1^1 \\ \tilde{c}_2^{-2} \\ \tilde{c}_2^{-1} \\ \tilde{c}_2^0 \\ \tilde{c}_2^1 \\ \tilde{c}_2^2 \\ \vdots \end{pmatrix} = \begin{pmatrix} D_{0(1\times1)} & & & \\ & D_{1(3\times3)} & & \\ & & D_{2(5\times5)} & \\ & & & \ddots \end{pmatrix} \begin{pmatrix} c_0^0 \\ c_1^{-1} \\ c_1^0 \\ c_1^1 \\ c_2^{-2} \\ c_2^{-1} \\ c_2^0 \\ c_2^1 \\ c_2^2 \\ \vdots \end{pmatrix} \qquad (10)$$

Where:

$$D_{mn}^l(\alpha,\beta,\gamma) = e^{-i\gamma n} . d_{mn}^l(\beta) . e^{-i\alpha m} \qquad (11)$$

$$d_{mn}^l(\beta) = \sum_{t=\max(0,n-m)}^{\min(l+n,l-m)} (-1)^t \frac{\sqrt{(l+n)!(l-n)!(l+m)!(l-m)!}}{(l+n-t)!(l-m-t)!(t+m-n)!t!} \times \left(\cos\frac{\beta}{2}\right)^{(2l+n-m-2t)} \left(\sin\frac{\beta}{2}\right)^{(2l+m-n)} . \qquad (12)$$

Matching quality is measured $\sqrt{MSD}$ by in equation 8 between model and template, directly from SPHARM coefficients [5]. Then, we obtain landmarks in template and datasets automatically by using nearly uniformed icosahedrons subdivision of spherical surfaces (figure 4).

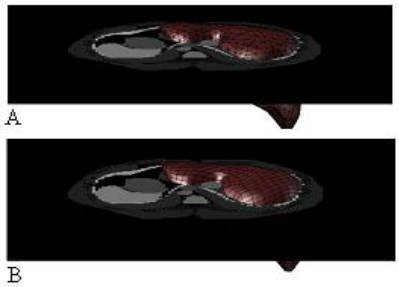

Figure 4. Landmark sampling: The liver of zubal phantom before (A) and after uniform sampling (B).

RESULTS

Landmark selection was performed by using mathematical operation in each case. An example of the landmark selection for liver and phantom are shown in (figure 5-a). Then, the registration step was done by applying TPS. The results of original and individual reconstructed phantom are also shown in (figure 5-b).

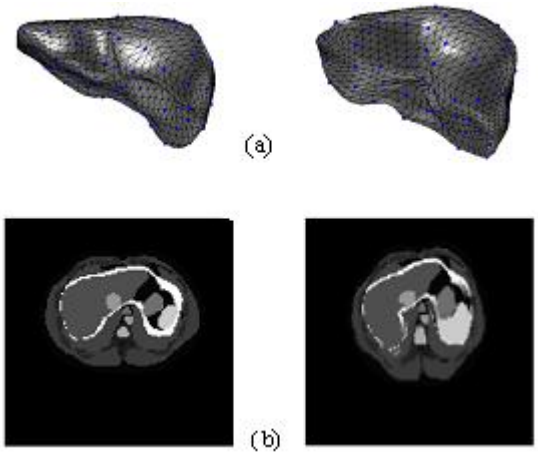

Figure 5. (a) The liver of phantom (left) and an example (right) with corresponding points by proposed method. (b) The slice of original phantom (left) and individual phantom (right).

The Hausdorff distance was selected as a metric parameter to evaluate our proposed method. It measures the distance between two subsets of surface, or point. Generally, the Hausdorff distance can be calculated from two sets [11], as follow:

Distance d(p,S) between a point p belongs to a surface S and a surface S as:

$$d(p, S') = \min_{p' \in S'} \|p - p'\|_2, \qquad (13)$$

where $\|\cdot\|_2$ denotes the usual Euclidian norm. The Hausdorff distance is the maximum distance of a set to the nearest pointing the other set. The Hausdorff distance between surface s and surface S' is given by:

$$d(S, S') = \max_{p \in S} d(p, S'), \qquad (14)$$

This distance is asymmetric, and in general $d(S,S') \neq d(S'',S')$. The distances $d(S,S')$ and $d(S'',S')$. are called forward and backward distance, respectively. The symmetrical Hausdorff distance defined as follows:

$$d_s(S,S') = \max(d(S,S'), d(S',S)). \qquad (15)$$

Reducing Hausdorff distance will indicate better registration method used. To have a comparison, criteria for we have used similarity index which demonstrated the percentage of reduction after applying the registration method. The Hausdorff distance for five livers, before and after applying proposed technique, were calculated according to the above mentioned method, and they are listed in table 1.

DISCUSSION

The first heterogeneous anthropomorphic model was devised at Oak Ridge National Laboratory for the Medical Internal Radiation Dose (MIRD) Committee of The Society of Nuclear Medicine [13, 14]. This model, known as MIRD Phantom, was based on the concept of the "Reference Man" for radiation protection purposes, although it was recognized that variation among individuals could be significant [15].

The medical community has already started using advanced imaging techniques, such as computed tomography (CT) and magnetic resonance imaging (MRI) to study patient specific anatomy. These new technologies suggest new types of body models for health physics dosimetry that are image-based and realistic.

A computational framework is presented by authors for constructing a three-dimensional individual computed tomographic phantom for liver structure using Zubal phantom. A novel automatic alignment method is explained for constructing the individual comparable phantom based on Coherent Point Drift (CPD) [7, 8], and spherical harmonics shape descriptors (SPHARM) [5], which is a powerful mathematical tool for analyzing and synthesizing the closed surfaces and human object shapes.

Table 1. Relative Hausdorff distance for five individual phantoms.

Case #	*1*	*2*	*3*	*4*	*5*	**Average**
Before-Registration	164.1	185.4	192.1	140.9	177.2	**171.94**
After-Registration	57.5	63.3	76.7	61.4	52.5	**62.28**
Similarity (%)	**%64.96**	**%65.86**	**%60.07**	**%56.42**	**%70.37**	**%63.78**

The visually verifying the proposed method is shown in figure 5 and Hausdorff distance and similarity index were selected also for quantity evaluation. The similarity between phantom and real liver can be increased up to %70. The results showed that the proposed method is effective for automatic individual phantom construction.

By this new, innovating technique, it is possible to adjust an existing standard phantom for each person, and we demonstrated how the liver can expand by point to point correlation. This preliminary study needs further evaluation by some experimental works using the proposed approach for dose calculation.

REFERENCES

1. Wernick MN and Aarsvold JN (2004) Emission Tomography. The fundamentals of PET and SPECT, Elsevier.
2. Park S, Lee JK, Lee C (2006) Development of a Korean adult male computational phantom for internal. *Dosimetry Calculation,* ***121:*** *257-264.*
3. Zubal IG, Harrell CR, Smith EO, Rattner Z, Gindi G, Hoffer PB (1994) Computerized three-dimensional segmented human anatomy. *Medical Physics,* ***21:*** *299-302.*
4. Saito K, Wittmann A, Koga S, Ida Y, Kamei T, Funabiki J, Zankl M (2001) Construction of a computed tomographic phantom for a Japanese male adult and dose calculation system. *Radiat Environ. Biophys,* ***40:*** *69-76.*
5. Shen L, Farid H, McPeek MA (2009) Modeling 3-dimensional morphological structures using spherical harmonics. *Evolution,* ***63:*** *1003-1016.*
6. Babapour F, Abbaspour A, Zoroofi R, Akhlaghpoor S (2008) Volumetric Non-rigid Registration via Thin-plate Spleen Model. *APCMBE,* ***19:*** *269–272.*
7. Myronenko A, Song XB, Carreira-Perpinan MA (2006) Non -rigid point set registration: Coherent Point Drift. *Proc NIPS, 1009-1016.*
8. Chui H and Rangarajan A (2003) A new point matching algorithm for non-rigid registration. *Computer Vision and Understanding,* ***89:****114-141.*
9. Besl PJ and Mckey ND (1996) A method for Registration of 3-D Shape. IEEE Trans. *Pattern anal Machine,* ***14:*** *239-256.*
10. Brechbuhler C, Gerig G, Kubler O (1995) Parameterization of closed surfaces for 3D shape description. CVGIP: *Image Understanding,* ***61:*** *154-170.*
11. Huttenlocher DP and Kedem K (1990) Computing the minimum hausdorff distance for point sets under translation. *Symposium on Computational Geometry, 340-349.*
12. Gonzalez RC and Woods RE (2002) Digital Image Processing (second edition) Prentice-Hall.
13. Snyder WS et al.(1978) Estimates of absorbed fractions for monoenergetic photon sources uniformly distributed in various organs of a heterogeneous phantom. MIRD Pamphlet No. 5, Revised (New York, NY: Society of Nuclear Medicine) .
14. Eckerman K Cristy E Ryman J (1996) The ORNL mathematical phantom series. (Oak Ridge National Laboratory, Oak ridege, TN) .
15. International Commission on Radiological Protection. (1975) Report on the Task Group on Reference Man. ICRP Publication 23 (Oxford: Pergamon press) .